Centrifuge modelling of piled foundations in swelling clays

Author 1

- T.A.V. Gaspar, PhD (Pretoria) – corresponding author
- Department of Civil Engineering, University of Pretoria, Pretoria, South Africa
- https://orcid.org/0000-0002-3746-2714
- Present address:
    - Department of Civil and Structural Engineering, University of Sheffield, United Kingdom
    - Sheffield, S1 3JD

Author 2

- S.W. Jacobsz, PhD (Cantab)
- Department of Civil Engineering, University of Pretoria, Pretoria, South Africa
- https://orcid.org/ 0000-0002-7439-2276

Author 3

- G. Smit, PhD (Southampton)
- Department of Civil Engineering, University of Pretoria, Pretoria, South Africa

Author 4

- A.S. Osman, PhD (Cantab)
- Department of Engineering, Durham University, United Kingdom
- https://orcid.org/0000-0002-5119-8841

Full contact details of corresponding author

- Email address 1: t.a.gaspar@sheffield.ac.uk
- Email address 2: tav.gaspar@gmail.com
- Mobile: +447488560650

Abstract

A study aimed towards assessing the variation in shaft capacity of piled foundations in swelling clays is presented. At the clay's in-situ water content, the results of pull-out tests on short length piles revealed no dependency of shaft capacity on overburden stress. Conversely, after achieving a targeted value of swell, a strong dependency on overburden stress was observed. In upper portions of the profile where swell can occur relatively freely, swell-induced softening results in a reduction in pile shaft capacity. However, at greater depths where swell is largely suppressed, so too are the effects of swell-induced softening. For this reason, shaft capacity at depth was found to remain relatively constant before and after swell. The results of an instrumented pile test revealed an overriding dependency of lateral induced swell pressure on the magnitude of heave which has occurred. Irrespective of the level of overburden stress, lateral pressures against the pile were found to increase at early stages of the swelling process, but then reduce as swell continued and softening began to occur. Such a result highlights the importance of specifying the level of swell at which shaft capacity should be assessed if a conservative design is to be obtained.

Keywords: expansive soils; centrifuge modelling; piles & piling; partial saturation

List of notations

e void ratio

N centrifuge model scaling factor

$\bar{p}$ net-mean stress

s suction

S_r degree of saturation

Number of words (text + 250x(tables+figures)): 9786

Number of figures: 15

Number of tables: 3

Introduction

The severe economic implications associated with construction on expansive clays (Jones & Holtz, 1973; Jones & Jefferson, 2012) have necessitated the implementation of specialised foundation solutions. Measures taken to mitigate the effects of this problem soil can broadly be divided into three categories, namely soil treatment or replacement, construction directly on the expansive profile and, isolation of the superstructure from the expansive profile.

Removal and replacement is generally a feasible approach if the depth of expansive material is shallow (approximately 2 m deep) and when suitable inert material is readily available (Byrne *et al.*, 2019). Alternatively, the soil can be 'treated' by pre-wetting the profile such that swell occurs before construction, thus limiting structural distress. Drawbacks of this approach include the time taken for the soil to reach an equilibrium moisture content, and the uncertainty of future changes in moisture throughout the lifetime of the structure (Byrne *et al.*, 2019). Arguably the most common approach for foundation design on swelling clays is to utilise a stiffened raft foundation (Byrne *et al.*, 2019; Charlie *et al.*, 1985; Li *et al.*, 2014; Pellissier, 1997). The rationale behind such a foundation type is to prevent differential movements across the foundation, thereby limiting structural distress. Isolation of the superstructure from the underlying expansive soil is the most expensive of the three approaches mentioned. The approach typically involves the use of piled foundations extending either to bedrock where they can be socketed, or to a stable soil horizon where the foundation can be anchored using, for example, enlarged base piles (Byrne *et al.*, 2019). These piles are then used to support a suspended foundation which is completely isolated from the underlying soil. The gap provided between the suspended foundation and the ground level provides space for the soil to swell into, without affecting the superstructure.

Piles used in this construction method can be subjected to large uplift forces due to heaving soil around the pile. To ensure cracking of the piles does not occur, they can either be adequately reinforced, 'sleeved' (provided with a slip layer) or a combination of these measures can be implemented (Fleming *et al.*, 2009). However, in cases where the expansive profile is particularly deep, 'sleeving' and/or socketing into bedrock can become uneconomical. In Kimberley, South Africa, expansive profiles have been found to extend to a depth of up to 30 m (Byrne *et al.*, 2019). Other instances of deep expansive profiles have also been reported in Sudan, where it is not uncommon to have expansive profiles extending to greater than 10 m (Elsharief, 2012).

While this foundation type can double the cost of construction (Jennings & Kerrich, 1962), if applied correctly, it can result in almost no foundation movements. This foundation type is however, not necessarily a fail-safe approach. Under-prediction of heave can result in the gap between the clay and suspended foundation swelling closed, thereby resulting in uplift of the superstructure.

A case study where such a design proved to be inadequate was reported by Meintjes (1991). The study reported structural damage due to excessive heave, despite the foundation being designed to have a void of 150 mm between the grade beam and pile cap, and under-reamed/enlarged base piles extending to a depth of 7.7 m.

Blight (1984) presented the findings of another case study where suspended foundations were used for several buildings at a thermal power plant. While the initial heave calculated for this site was in the order of 120 mm (Blight, 1984), this was a gross underestimation of what was observed. Prior to construction, removal of vegetation resulted in rising of the water table, causing far greater heave than what was initially estimated, thereby closing the gap between ground level and the suspended foundation. Some remedial measures implemented at this site have involved increasing the gap between the suspended slabs and the expansive clay

to 300 mm. It has been noted that at some buildings at the power plant, these voids have swelled closed yet again (Day, 2017).

This particular case study led to a number of useful investigations on this method of construction. Blight (1984) conducted full-scale pull-out tests on short length piles before and after wetting the profile for a period of 3‑4 weeks. His results indicated that an increase in pile pull-out (shaft) capacity was observed after wetting. This finding was in direct contradiction with a study conducted by Elsharief *et al.* (2007) for pile load tests conducted in Sudan. An explanation for this contradiction is that, while the swelling process can produce an increase in lateral stresses against a pile shaft, swell induced softening of the clay (Gens & Alonso, 1992) results in a reduction of shear strength which can ultimately reduce shaft capacity. This softening can be viewed as resulting due to a reduction in matric suction, or the structural realignment occurring due to macroscopic volumetric change (i.e. swell) (Gens & Alonso, 1992). If an engineer is to produce a conservative design for such foundation types, an understanding of these counteracting mechanisms is crucial.

In an effort to investigate the effects of these mechanisms, Smit *et al.* (2019) presented the results of centrifuge pile pull-out tests. The study involved pull-out tests of bored piles installed in an expansive profile at:

a) the clay's in-situ water content and
b) after allowing swell to occur.

The results of this study indicated that, after achieving a targeted magnitude of swell, the pull-out capacity of piles reduced by between 57 and 67% when compared to their capacities at the clay's in-situ water content.

While the results of this preliminary study indicate average shaft friction along the full length of the pile, they give no information on the variation in shaft (pull-out) capacity with depth. Furthermore, such tests investigate the consequence of the two counteracting mechanisms (softening and changes in lateral stresses) without measuring these quantities directly. This study presents a series of centrifuge models aimed to address these shortcomings and provide insights into the aforementioned counteracting mechanisms.

The first three tests presented in this study involve pull-out tests conducted on short length piles (plugs) at various depths throughout the clay profile. The intention of these tests is to investigate the effect of confinement on the evolution of pile shaft capacity before and after swell. The final test incorporates the use of an aluminium pile, instrumented to measure the change of lateral pressures on the pile shaft throughout the swelling process. This instrumented pile test also included in-flight penetration tests at the clay's in-situ moisture content and after allowing swell to occur. The purpose of this strength characterisation was to obtain an indication of the magnitude of swell-induced softening.

Basic soil classification

The material tested in this study was a highly expansive clay, sampled from the Limpopo province of South Africa, 350 km northeast of Pretoria. The material was sampled from the upper 1.5 m of the profile and can be described as a stiff, fissured and slickensided black clay containing fine nodular calcrete (Day, 2020).

Basic classification tests were performed to establish the soil's particle size distribution (by method of sieving (ASTM, 2017a) and hydrometer (ASTM, 2017b)), Atterberg limits (ASTM, 2017c) and specific gravity (ASTM, 2014a). These results, as well as the unified soil classification (ASTM, 2017d) are presented in Fig. 1 and Table 1. X-ray diffraction testing to determine the mineralogical composition of the clay was performed on the same site by a previous researcher, the results of which are shown in Table 2

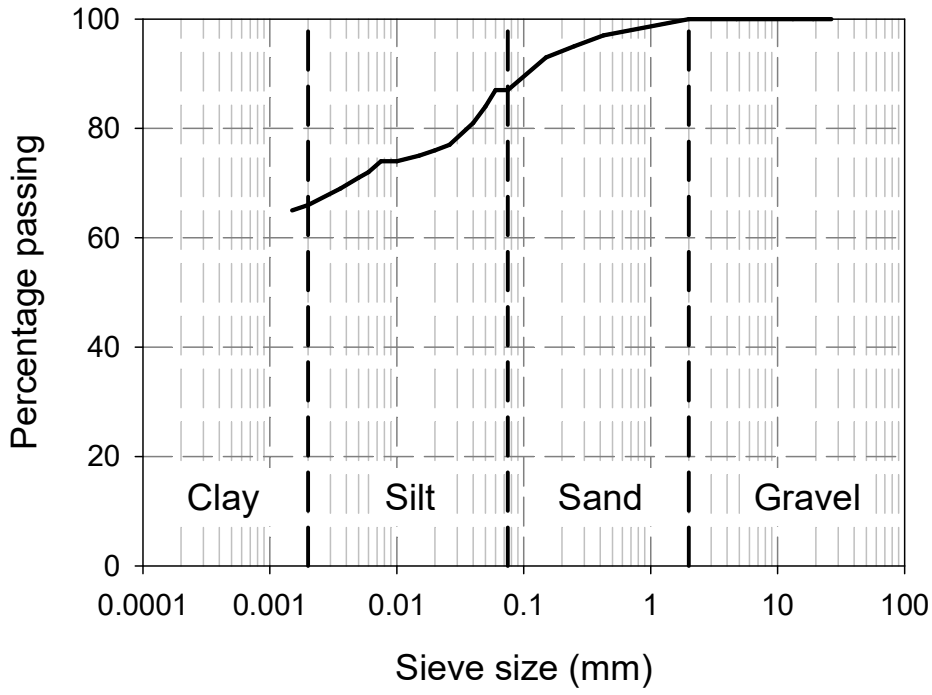

Fig. 1. Particle size distribution

Table 1. Soil classification data

Liquid limit (%)	92
Plasticity index	55
Linear shrinkage (%)	25.5
Activity	0.8
Specific gravity	2.65
Unified soil classification	CH

Table 2. Mineralogical composition based on X-ray diffraction (after Moses, 2008)

Mineral	Composition (%)
Smectite	58
Palygorskite	19
Calcite	5
Plagioclase	5
Quartz	4
Enstatite	4
Kaolinite	3
Diopside	2

Characterisation of swell properties

The mechanical properties of both compacted and undisturbed samples of the clay considered in this study was presented by Gaspar *et al.* (2022). The following section presents a summary of the oedometer tests conducted to quantify the swell properties of the tested clay. For the swell tests, data is presented for both compacted and undisturbed specimens (prepared from block samples). In doing so, the extent to which the laboratory prepared specimens replicated the undisturbed swell behaviour could be assessed.

Recognising the difficulties associated with preserving the fissured macrofabric of expansive clays during the sampling process, the preparation procedure implemented was aimed towards introducing a certain degree of 'fissuring' for samples prepared in the laboratory. This was accomplished by breaking down intact lumps of clay with a cheese grater at their in-situ water content (approximately 31%) and statically compacting the broken-down clay to a targeted dry density of 1350 kg/m^3. These initial conditions were selected as they are representative of the measured in-situ properties of the clay after the dry season. The rationale for targeting properties related to this season is that they present the most critical case if swell

properties are to be measured (i.e. assessing the soil in its driest practical state allows for the largest estimates of swell magnitude and swell pressure to be obtained).

This preparation procedure differs slightly from more conventional approaches whereby air-dried soil is mixed with a predetermined quantity of water, allowed to equilibrate, and compacted to a target dry density (Monroy *et al*., 2015; Manca *et al.,* 2016). The drawback of this more conventional approach, however, is that it results in a fabric with macropores which are relatively isolated. This is in contrast to the fabric type more commonly associated with expansive clays which consists of a series of interconnected pores (i.e. fissures) that more easily facilitate the ingress of water.

To investigate the swell properties of the compacted and undisturbed specimens, a series of *wetting after loading tests* (ASTM, 2014b), sometimes referred to as *swell under load* tests, were conducted at various applied stresses. Such tests involve placing an unsaturated sample into the oedometer, applying a predetermined stress (referred to as the soaking stress) and then flooding the housing with distilled water. As the sample is inundated, volumetric changes are monitored until such point that these changes become negligible. Once volumetric changes cease, the sample is considered as having reached a state of zero suction (Schreiner, 1988) and the final volumetric strain is noted for that stress level. Table 3 presents the initial sample properties for the oedometer swell tests. Fig. 2 illustrates the results of wetting after loading tests for both the compacted and undisturbed specimens conducted at several values of applied vertical stress. Linear regression curves have also been superimposed onto the dataset for both the compacted and undisturbed samples.

Table 3. Initial sample properties for oedometer swell tests

Description	Soaking stress (kPa)	Void ratio, e	Gravimetric water content, w (%)	Degree of saturation, S_r (%)	Dry density (kg/m^3)
Compacted	12.5	0.969	33.6	91.9	1346
Compacted	25	0.971	33.6	91.6	1344
Compacted	50	0.908	30.3	88.5	1389
Compacted	100	0.938	32.2	90.9	1367
Compacted	200	0.973	34.6	94.4	1343
Compacted	300	1.037	34.6	88.6	1301
Compacted	400	1.027	34.6	89.4	1307
Undisturbed	12.5	0.939	31.5	89.0	1367
Undisturbed	25	0.888	30.3	90.5	1403
Undisturbed	50	0.817	29.5	95.6	1459
Undisturbed	100	0.889	30.2	90.2	1403
Undisturbed	200	0.901	29.9	87.8	1394
Undisturbed	300	0.992	30.3	81.0	1331
Undisturbed	400	1.020	32.0	83.2	1312
Undisturbed	500	1.068	30.8	76.3	1281

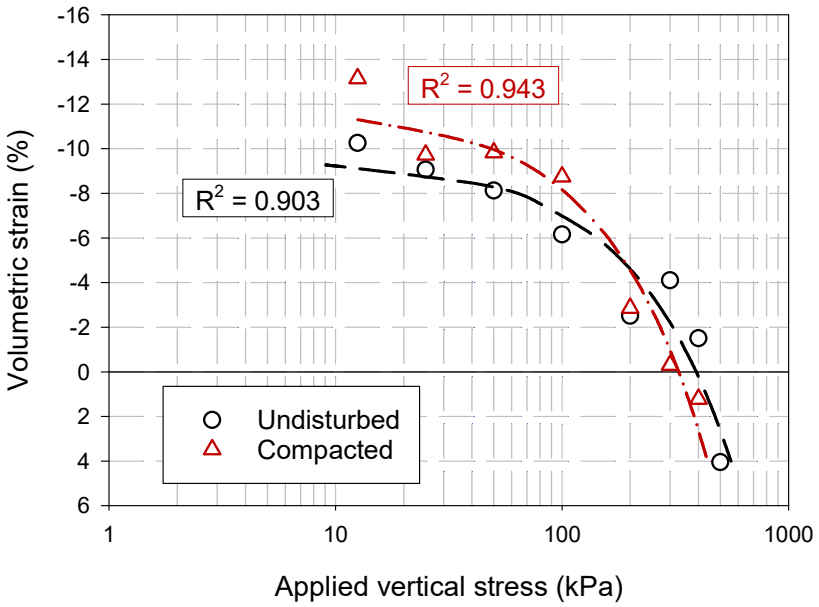

Fig. 2. Soaking under load curves for compacted and undisturbed samples

From Fig. 2 it can be seen that the measured swell properties of the compacted and undisturbed specimens are similar. Not only was the magnitude of swell achieved at all soaking stresses similar for the compacted and undisturbed samples, but the swell pressure also remained close. Using the regression curves plotted in Fig. 2, the stress required to achieve 0% volumetric change was 329 and 392 kPa for the compacted and undisturbed specimens respectively. Such results illustrate that the sample preparation procedure implemented was able to retain key swell characteristics of the undisturbed material. In light of this finding, the same approach was implemented in the preparation of the centrifuge models presented in the following section. It should also be highlighted that Gaspar et al. (2023) also reported the saturated hydraulic conductivity (k_{sat}) to be in the range of 10^{-9}-10^{-12} m/s. These values were obtained by applying consolidation theory ($k_{sat} = c_v . m_v . \gamma_w$) to calculate k_{sat} from a consolidation test on a sample reconstituted at 1.1 times the soil's liquid limit.

Model descriptions

This section provides details of the centrifuge tests conducted in this study. First, a description of the clay profile and its preparation is provided. Additionally, aspects of the model layout which are common to all tests are outlined. Thereafter, specific reference is made to the position of piles within the clay profile, as well as the sequence that was followed for each individual test. Unless otherwise stated, all dimensions provided in figures are in model scale. Full-scale (prototype) lengths can be obtained by multiplying model dimensions by the model scaling factor (N=30).

The centrifuge tests described in this study modelled an expansive soil profile comprising of a stack of 5 clay layers (50 mm thick), statically compacted to a targeted dry density and gravimetric water content of 1350 kg/m^3 and 31% respectively (the average in-situ values determined from site investigations). It should be noted that at this state, the clay layers had a matric suction of approximately 2 MPa. The clay layers were separated by needle punched, non-woven geotextiles. The inclusion of geotextiles in the centrifuge models presented is to facilitate the rapid ingress of water. Additionally, the geotextiles were sized such that hydraulic contact could be maintained between geotextiles separating the clay layers, and the adjacent water wells (described at the end of this paragraph). By controlling the length of the respective geotextiles, an effort was made to avoid any anchorage of the geotextiles at their ends such that they were able to move freely in the vertical direction as swell occurred, and not provide stiffness to the profile. The five clay layers were laterally restrained in position by two perforated steel plates, covered with the same geotextile used to separate the clay layers. The two spaces on either side of the model were used as water wells to facilitate the ingress of water. All tests presented in this study were performed at a centrifugal acceleration of 30 g.

The layout of the first two tests presented in this study, shown in Fig. 3, were identical and incorporated 4 short-length piles (plugs) installed at various depths. For Test 1, the plugs were pulled out of the profile at the clay's in-situ water content. In this study the "pull-out" capacity

is defined as the force required to mobilise peak shaft resistance between the bored piles and surrounding clay. Water was subsequently introduced into the strongbox through inlets at the bottom of the model until the water level was approximately 20 mm above the surface of the top layer. Once the flooding process was complete, every clay layer had access to water on all four boundaries (top, bottom and sides). The front and back of the model were confined between the strongbox's glass window and an aluminium partition plate. After achieving the targeted value of swell, ≈ 6.8 mm model scale, (as predicted by the Van der Merwe (1964) empirical prediction method for a clay of *very high potential expansiveness*), the plugs were pulled for a second time.

For the second test presented, pull-out tests were only conducted after the targeted swell was achieved. From Fig. 3 it can be seen that the augered holes above the short length piles were unsupported. As a result, clay was able to swell behind the plug as the strongbox was flooded. To investigate the effect of the augered holes swelling closed above the plugs, a final pull-out test was conducted whereby an aluminium tube was used to support the holes during swell (all other aspects of the model layout remaining unchanged). The plugs were then pulled out at the same magnitude of vertical swell as was done for the previous tests. An illustration of the augered hole support is presented in Fig. 4. As shown in Fig. 4, a gap of 5 mm was left between the top of the piles and the aluminium tube. The purpose of this gap was to ensure a that the peak shaft resistance of the piles could be mobilised before making contact with the supporting tube. Furthermore, the tube was clamped at the surface to ensure that this gap was maintained, even as the soil swelled.

For all three pull-out tests, plugs were cast from a rapid hardening grout with a 4 mm stainless steel threaded rod at their centres. Comparisons of material properties of this grout with a scaled concrete mix developed for centrifuge modelling (Louw *et al.* 2020) indicated that the two materials had similar mechanical properties (Gaspar, 2020). Furthermore, the load and displacement of piles throughout testing were monitored using load cells and linear variable

differential transformers (LVDTs) respectively in all three tests. It should be noted that for all three pull-out tests, each short-length pile in a given model was pulled out individually (rather than all piles in a model being pulled at the same time). It was therefore possible to ensure that the testing of a single pile did not induce displacements throughout the model which might affect testing of adjacent piles. Additionally, LVDTs were also used to measure swell magnitude at the surface of the clay profile.

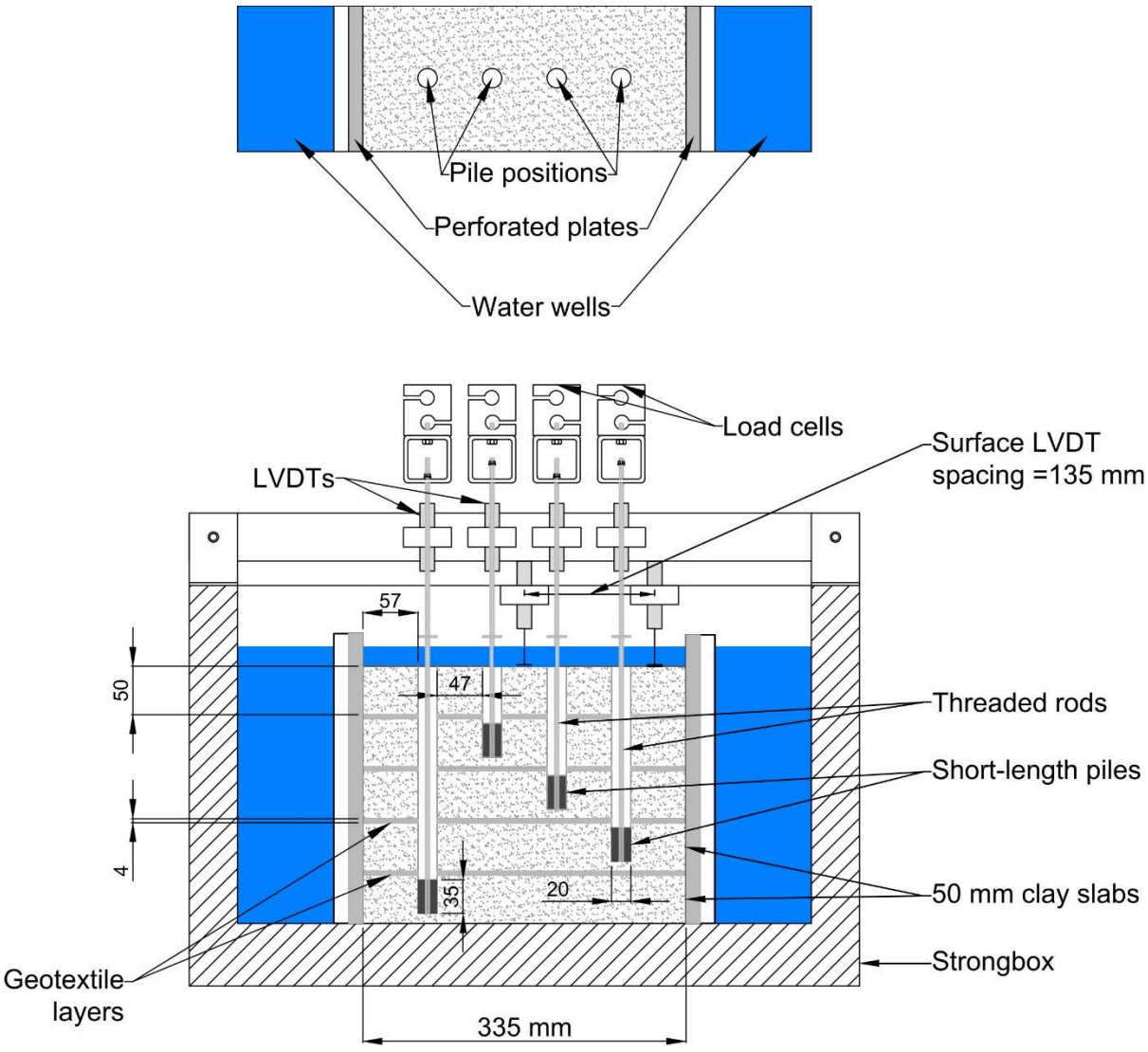

Fig. 3. Model layout for Tests 1 and 2

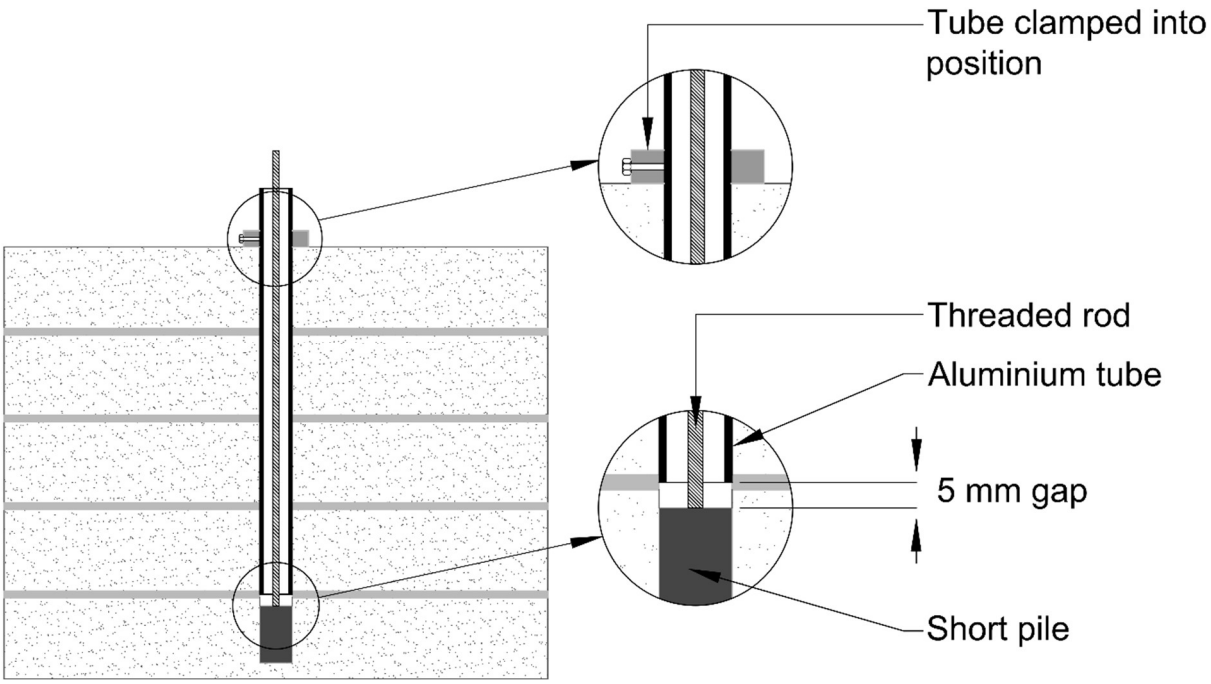

Fig. 4. Setup used to support augered holes behind piles

The layout of the final test is illustrated in Fig. 5. The test consisted of a single aluminium pile in the centre of the model (anchored at its base), instrumented with lateral load cells positioned at the centre of each clay layer. Measuring 19.05 mm in diameter, the pile was placed in a thin latex membrane to protect instrumentation from the water that would ultimately be introduced into the strongbox. The pile was then inserted (from the top of the profile) into an augered hole with a 20 mm diameter.

For the instrumented pile, the lateral load cells used were designed, based on an approach suggested by Jacobsz (2002). The load cells were manufactured from aluminium using a process referred to as electrical discharge machining (EDM). As shown in Fig. 6, the load cells comprised of two rounded surfaces and an inner web measuring 0.3 mm in thickness. This web was instrumented on either side with 1 kΩ strain gauges and wired into a full-Wheatstone bridge configuration. Once slotted into the aluminium pile, the rounded edges of the load cells fitted flush with the outer diameter of the pile as illustrated in Fig. 7.

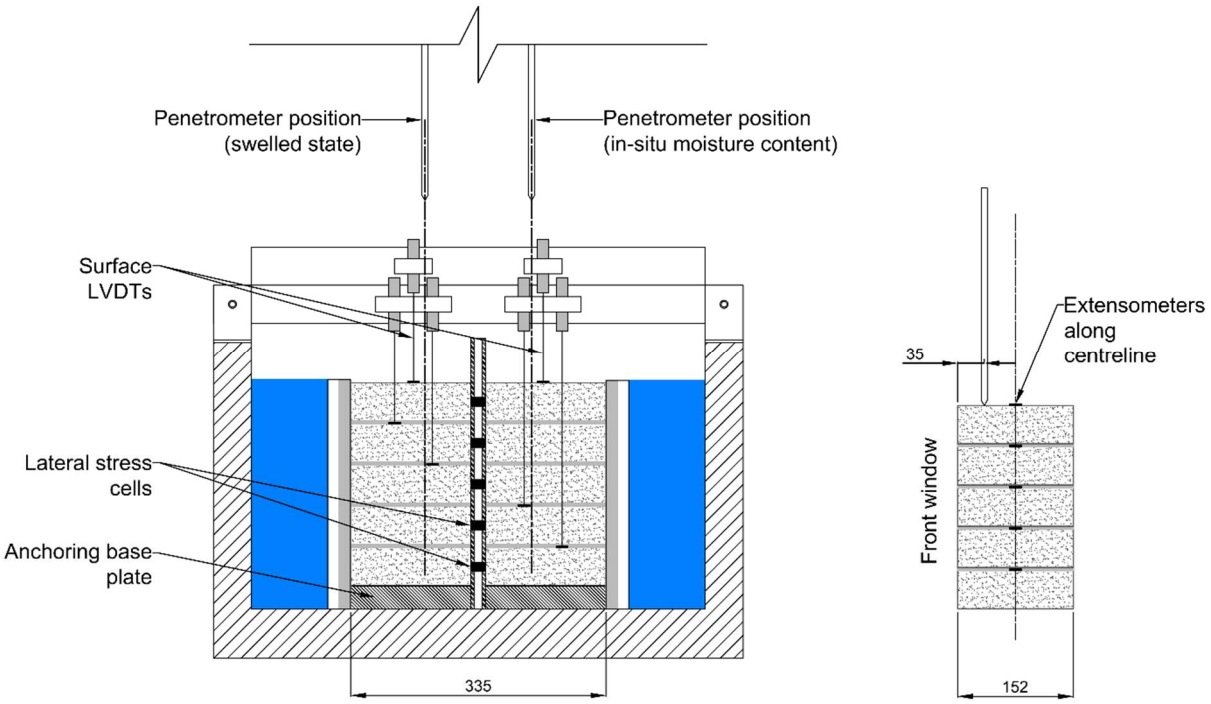

Fig. 5. Instrumented pile test

Fig. 6. Un-instrumented lateral load cells

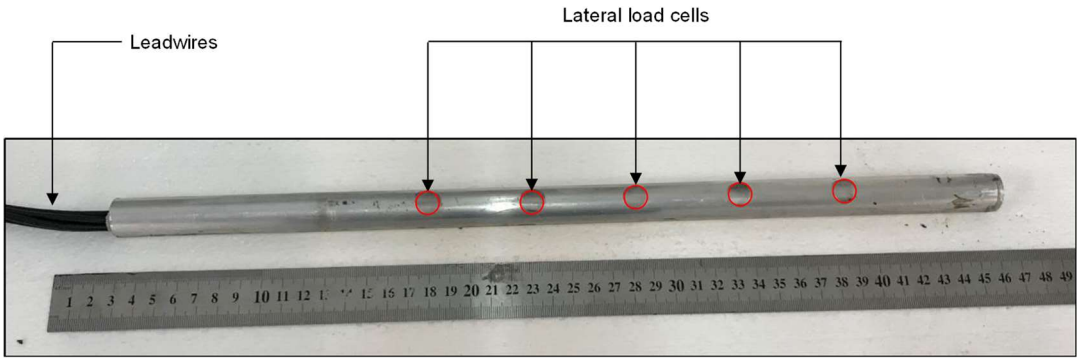

Fig. 7. Assembled instrumented pile

This test sequence involved accelerating the model to the desired centrifugal acceleration of 30 *g* at the clay's in-situ water content. The strongbox was then flooded with water, inducing swelling of the profile. Throughout the swell process, changes in lateral stresses against the pile shaft were monitored. Additionally, strength measurements of the profile were performed in-flight by means of cone penetration testing (CPT). CPTs were performed at the clay's in-situ water content, and after the targeted swell magnitude had been achieved (that predicted by Van der Merwe (1964) for a clay of *very high potential expansiveness*). The CPT measurements for this test are presented in Fig. 8. Also included in Fig. 8, are CPT measurements conducted in a greenfield centrifuge test (i.e. considering only a soil profile with no external structures or loads) conducted on the same soil type for the same model layout (Gaspar *et al*., 2023).

While holes were cut in the geotextiles to provide a path for the penetrometer to pass through, the penetrometer punched through the bottom two geotextile layers during the instrumented pile test, as indicated in Fig. 8. In Fig. 8 the prefixes "GF" and "IP" in the legend indicate the greenfield and instrumented pile tests respectively.

From this figure, it can be seen that the penetration resistance reduced substantially during the swell process. Furthermore, CPTs performed at the clay's in-situ water content and after achieving the targeted swell are similar for the instrumented pile test and the greenfield test. This finding provides confidence that the sample preparation procedure implemented for these two tests, as well as for the pull-out tests discussed previously, produced specimens with consistent strength. Similarly, it illustrates that any tests performed after achieving the targeted swell were also carried out under comparable conditions. Key details of the four centrifuge tests conducted are highlighted in Table 4.

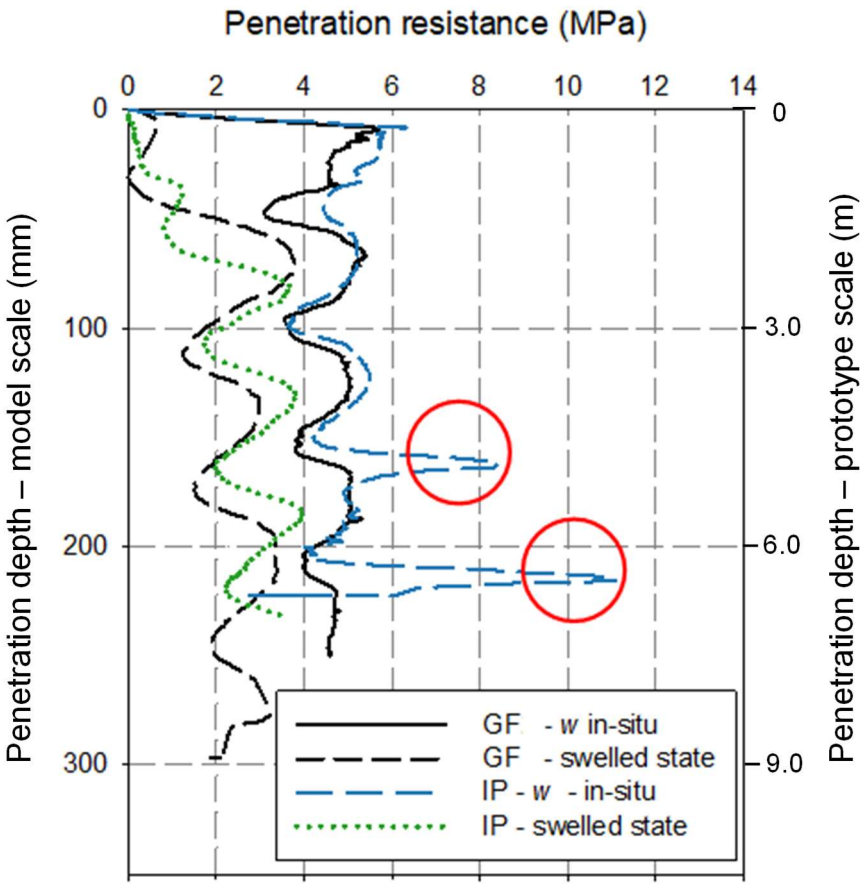

Fig. 8. Penetration results for the greenfield (GF) (after Gaspar *et al.* (2023)) and instrumented pile (IP) tests

Table 4: Test program

Test ID	Pile material	Pile dimensions (model) – length (L); diameter (D) (mm)	Pile dimensions (prototype) – length (L); diameter (D) (m)	Testing period
T1	Rapid hardening grout	L = 35 D = 20	L = 1.05 D = 0.6	Before and after swell
T2	Rapid hardening grout	L = 35 D = 20	L = 1.05 D = 0.6	After swell
T3_S	Rapid hardening grout with aluminium tube supporting holes	L = 35 D = 20	L = 1.05 D = 0.6	After swell
T4_I	Aluminium (instrumented)	L = 355 D = 19	L = 10.65 D = 0.57	From in-situ water content, throughout swell process

Results

The results presented by Smit *et al.* (2019) revealed that the pull-out (shaft) capacity of full-length piles reduced after allowing swell to occur. The aim of the plug pull-out tests was to investigate the dependency of plug pull-out capacity on confinement (overburden) stress at various depths.

Plug pull-out capacity (Test 1)

This series of pull-out tests aimed to investigate the pull-out capacity of piles prior to swell, i.e. at the soil's in-situ water content. After obtaining the pull-out capacity of the plugs at their in-situ water content, the model was flooded to allow the targeted swell to be achieved. Once reached, the plugs were pulled a second time. Fig. 9 illustrates the mobilised shaft friction versus plug displacement during the pull-out tests, prior to and after swell.

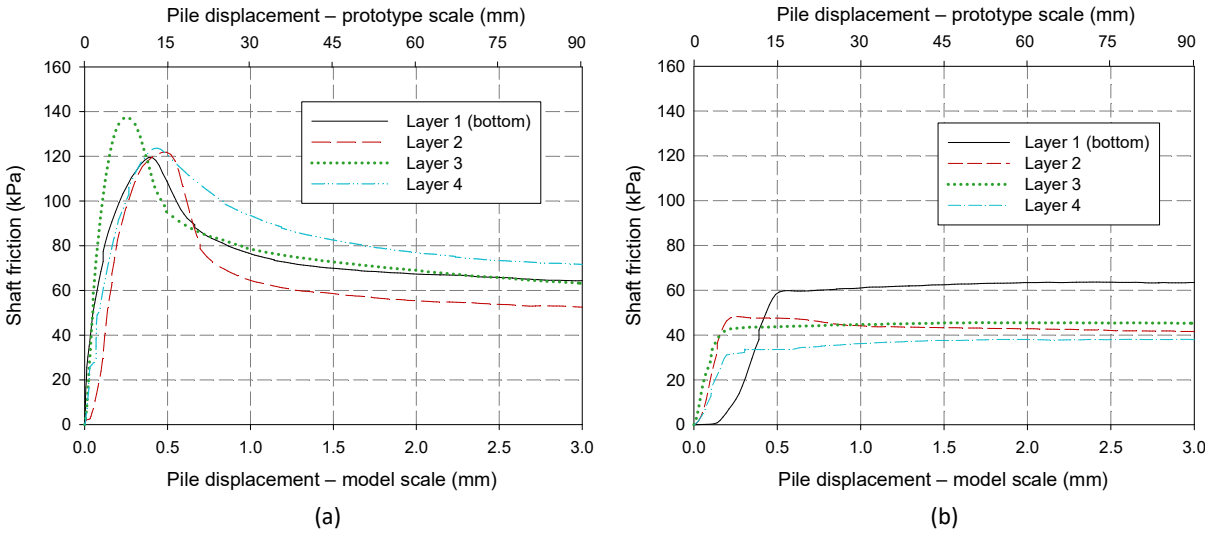

Fig. 9. Mobilised shaft friction versus pile displacement at a) the soils in-situ moisture content and b) after swell had occurred during pull-out tests

From Fig. 9a) it can be seen that peak shaft friction was achieved at approximately 0.4 mm (0.02 pile diameter) displacement for all plugs except that in Layer 3, which reached its peak at approximately 0.25 mm (0.0125 pile diameter). Fig. 9a) illustrates that the peak shaft friction achieved appears independent of depth within the model and thus of confining pressure. Three of the piles consistently reached a peak shaft friction of approximately 120 kPa, with the plug in Layer 3 achieving a peak shaft friction of close to 140 kPa.

Fig. 9b) presents the pull-out results for the same plugs after the targeted swell had been reached. In this figure, no peak is observed, but rather all piles appear to reach a certain value of shaft friction and then remain constant. Since this figure presents the results of piles which were previously pulled out of the soil, it might be expected that the maximum shaft friction

attained with any further “pulling” would be equivalent to the residual value observed in Fig. 9a). This argument is supported by considering that a failure plane would already have been established during the first pull-out test. However, upon closer inspection, it can be seen that there are some differences between the maximum values of shaft friction attained in Fig. 9b) and the values of residual friction observed in Fig. 9a). These differences can be attributed to the softening that occurred during the swell process.

The largest difference is for the plug in the surface layer (Layer 4) where the lowest confining stress of the 4 plugs would have been experienced. The smallest difference was for the plug in Layer 1 at the bottom of the model (experiencing the highest confining stress). The result in Fig. 9 can be interpreted within the extended Barcelona Basic Model for Expansive Clays (BExM). For this interpretation, it is useful to consider Fig. 10 which highlights the stress state at various positions in the profile in relation to the load collapse (LC) yield curve. In this figure, all 4 layers begin at the same value of suction (s_i). The macroscopic expansion associated with the reduction in suction results in soil softening, which can be represented as the movement of the LC yield curve to the left. The extent of this movement is related to the position of the initial stress state relative to the LC curve. For lower net-mean stresses, the initial stress state is further from the LC curve and will therefore result in the most softening.

It should be noted that in Fig. 10, it has been assumed that the suction within the bottom 4 clay layers reduced by approximately the same amount. This is supported by the consistent CPT measurements for these layers as presented in Fig. 8. As overburden stress increases with depth, swell is incrementally restricted to a larger degree. For this reason, the magnitude of swell-induced softening becomes negligible in the bottom layer, where very little swell occurred. Conversely, in the top layer where the most swell was observed, the effects of swell-induced softening produced the differences between the residual shaft friction in Fig. 9a) and the peak shaft friction in Fig. 9b).

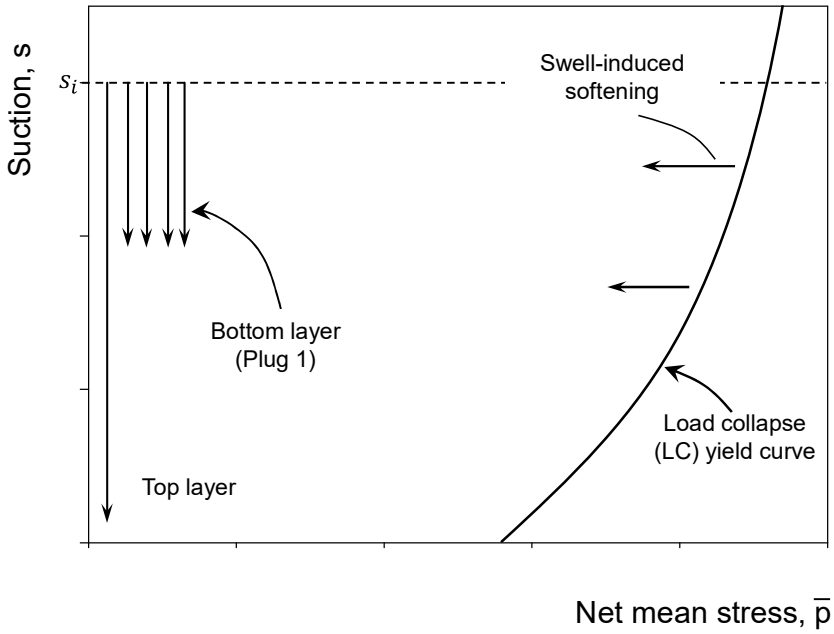

Fig. 10. Interpretation using the BExM framework

Plug pull-out (Test 2-after swell)

The model layout for Test 2 was identical to that presented in the previous section. However, for this test, plugs were only pulled once the targeted swell magnitude had been achieved, as opposed to pull-out at the in-situ moisture content in the previous test. Fig. 11 illustrates the results of this pull-out test.

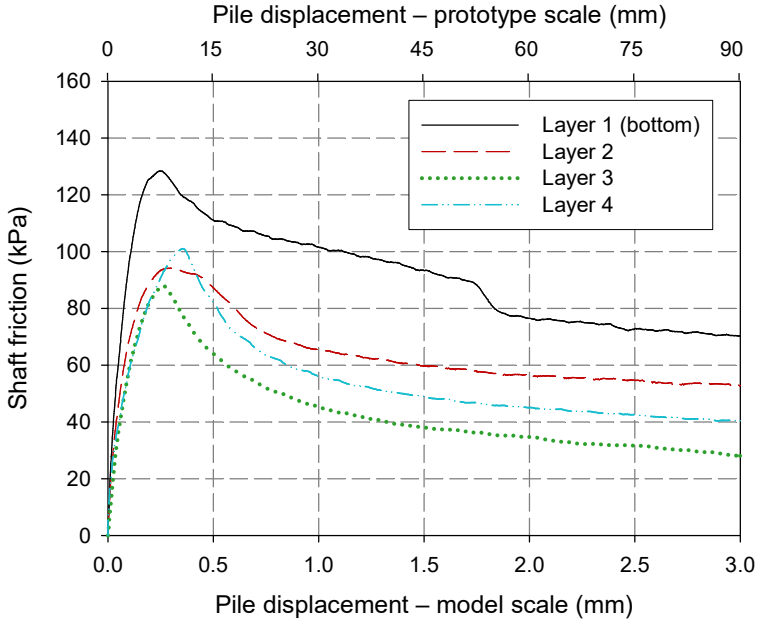

Fig. 11. Pull-out test after swell (unsupported holes)

In the study conducted on full-length piles by Smit *et al.* (2019), it was found that the pull-out (shaft) capacity reduced by approximately 60% following swelling. Similarly, the results presented in Fig. 11 show a reduction in shaft resistance for all layers, except Layer 1 (at the bottom of the model). In describing the possible mechanisms responsible for the observed increase in pull-out capacity after swell, Blight (1984) attributed his finding to an increase in lateral pressure against the piles. Conversely, Elsharief (2007) attributed the observed reduction in shaft resistance after wetting, to post-swell softening.

The results of the centrifuge models presented thus far illustrate that there is a relationship between overburden stress and the dominant mechanism governing pile shaft capacity after swell. Closer to the surface, swell is allowed to occur more freely, and so swell-induced softening is the dominant mechanism. At depth where swell is restricted by overburden stress, so too is swell-induced softening and, as such, shaft capacity remains relatively unchanged during and after the wetting process.

Fig. 12 illustrates a typical example of a plug just after being removed from the model. From this photo, it is evident that during a pull-out test, failure occurs within the clay rather than along the pile/soil interface as may be expected for a perfectly smooth (e.g. aluminium) pile. This observation is in agreement with what was observed by Smit *et al.* (2019).

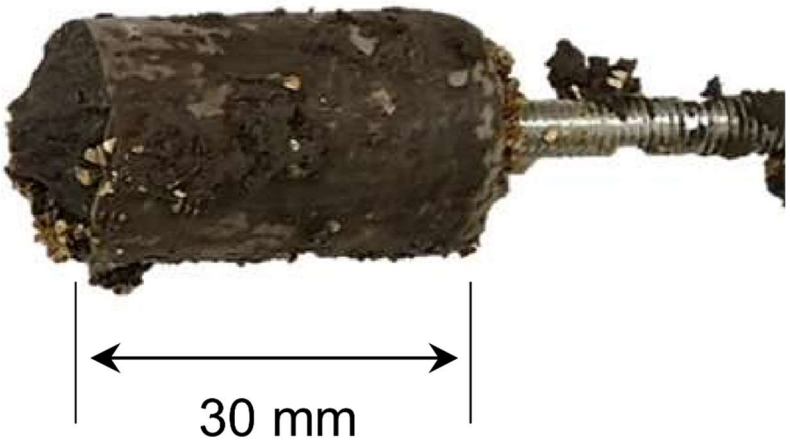

Fig. 12. Photograph of short length pile after being pulled out of a swelled profile

Plug pull-out (Test 3 – after swell - supported holes)

The final pull-out test had the same layout as the previous two tests, except for the fact that the holes above the plugs were supported with aluminium tubes. This test was performed to determine to what degree (if any) the clay which swelled above the plugs affected the measured pull-out (shaft) capacities. Fig. 13 presents the results of the two pull-out tests conducted after swell with and without supported holes.

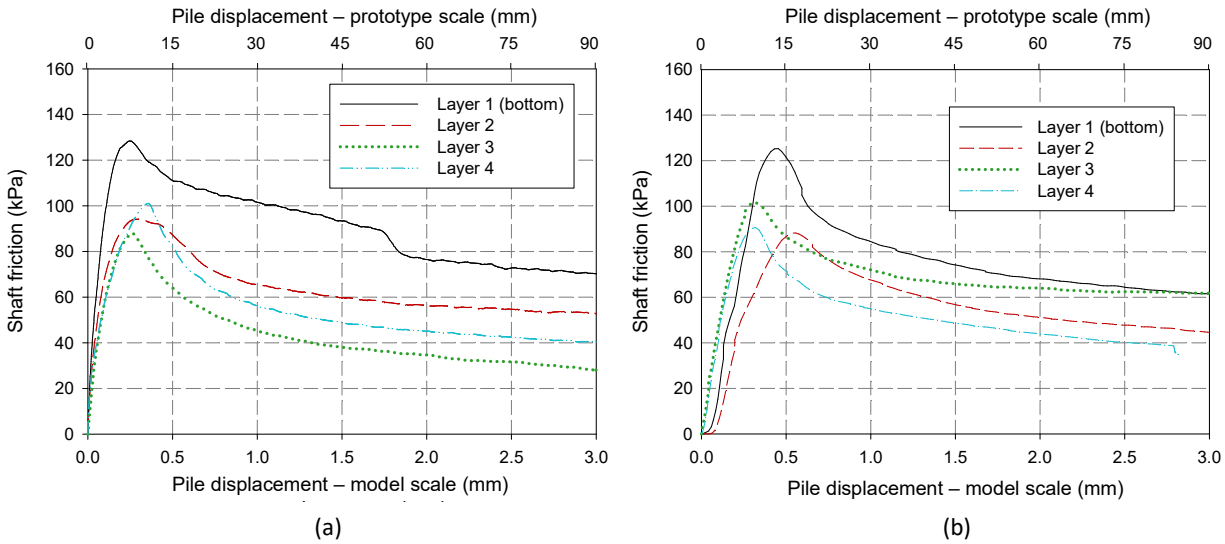

Fig. 13. Plug pull-out tests conducted after achieving the targeted swell for a) unsupported holes and b) supported holes

The result presented in Fig. 13 illustrates that the soil swelling above the plugs for the test with unsupported holes had a negligible effect on the measured peak shaft friction. This can be

attributed to the fact that the soil which was allowed to swell behind the plug had softened significantly.

Fig. 14 presents the results of peak shaft friction (i.e. pull-out capacity) for the various pull-out tests conducted. On the primary vertical axis (left) the overburden stress has been calculated from the initial unit weight of the various layers. The secondary vertical axis (right) illustrates the position of the plug as the height above the base of the model in model scale. A third vertical axis (far right) presents the height above the base of the model in prototype scale. The results of the pull-out tests have also been summarised in Table 5.

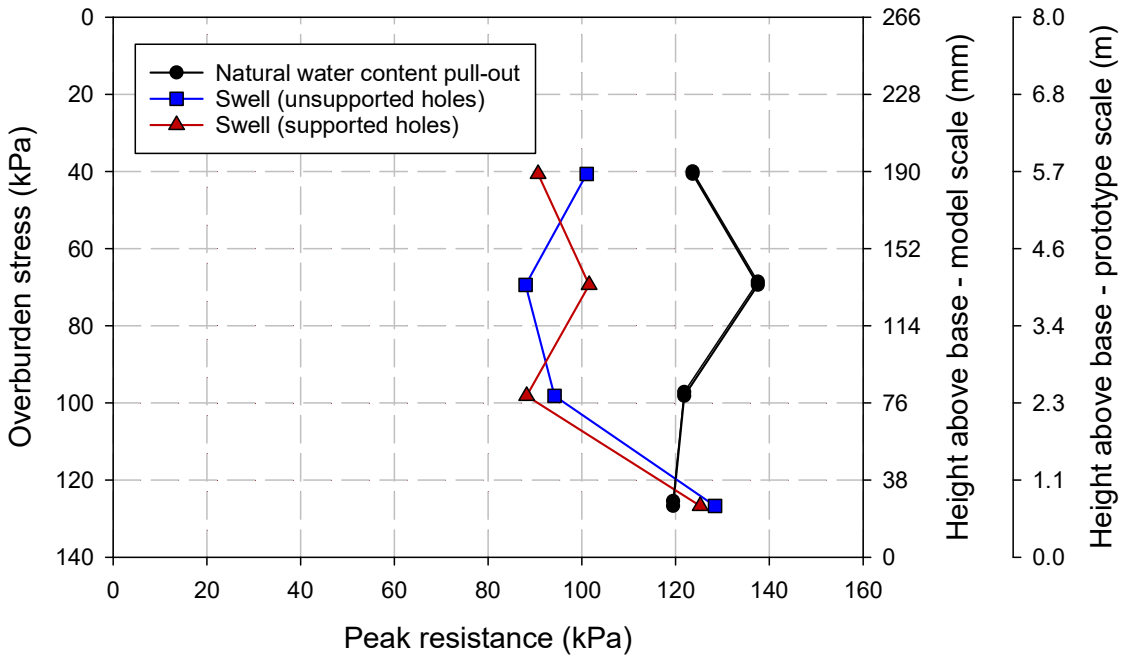

Fig. 14. Comparison of pull-out capacities for the various pull-out tests conducted

Table 5: Summary of pull-out test results

Test ID	Layer	Peak friction – before swell (kPa)	Residual friction – before swell (kPa)	Peak friction – after swell (kPa)	Residual friction – after swell (kPa)
T1	1	119.5	64.4	63.5	NA
	2	121.8	72.0	41.6	NA
	3	137.6	63.1	45.2	NA
	4	123.6	52.5	37.9	NA
T2	1	NA	NA	128.3	69.0
	2	NA	NA	94.3	52.7
	3	NA	NA	87.8	27.6
	4	NA	NA	101.0	39.9
T3_S	1	NA	NA	125.3	61.0
	2	NA	NA	88.2	44.3
	3	NA	NA	101.6	61.6
	4	NA	NA	90.7	38.8

The results in Fig. 14 illustrate that in general, there is a reduction in pull-out capacity of piles after allowing swell to occur. However, at high confining/overburden stresses, pull-out capacity appears to be unchanged (and may increase locally) since the restriction of vertical swell results in a reduction of swell-induced softening. Fig. 14 also illustrates good repeatability in test results for piles pulled out after achieving targeted swell.

Instrumented pile test

The purpose of this test was to measure changes in lateral swell pressure against the pile shaft throughout the swell process. It should be highlighted that after installation, there was a gap estimated at approximately 0.5 mm between the augered hole perimeter and the pile. As

a result, some expansion of the clay would have had to occur before contact was made with the pile. This is an important factor to recognise since any amount of heave can significantly reduce the magnitude of lateral swell-pressure against a structure (Fourie, 1991). For this reason, this test aimed to provide a qualitative illustration of the variation in swell pressure against the instrumented pile. The results of this test are provided in Fig. 15.

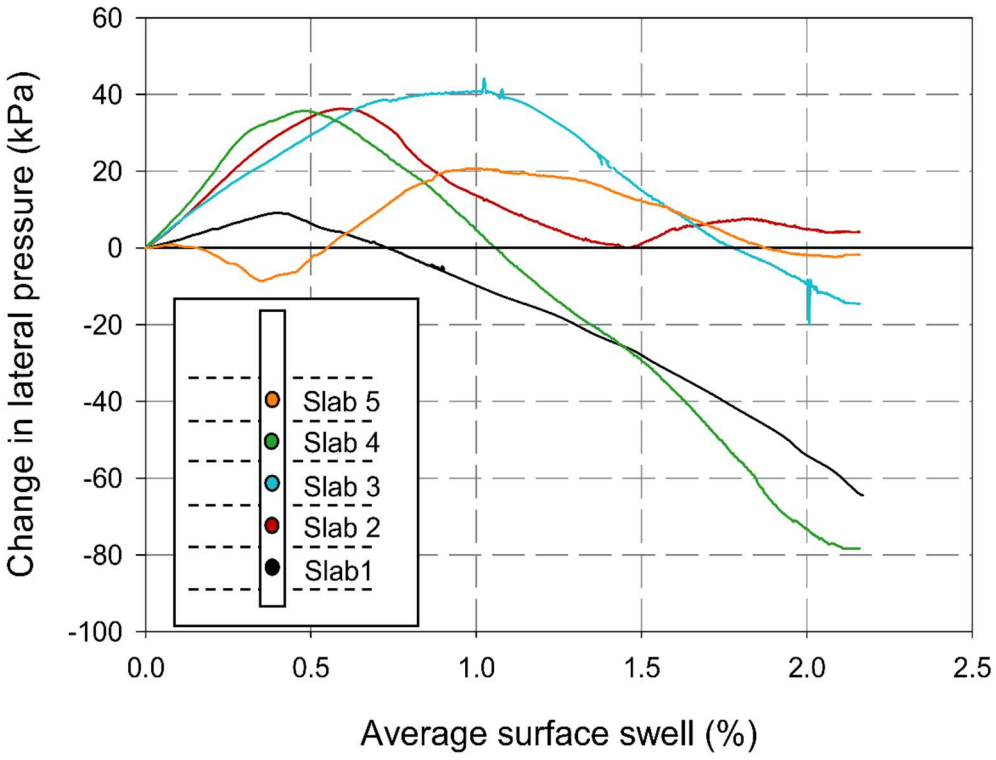

Fig. 15. Change in lateral pressure due to swell

The results presented in Fig. 15 illustrate the *change* in lateral swell pressure against the pile. Data in this figure was zeroed after the model had been flooded. The data presented extends from the instant that the water level within the strongbox had cleared the top of the surface of the profile to the point at which the targeted swell had been achieved.

From Fig. 15 it can be seen that the top layer initially experienced a slight reduction in lateral pressure, followed by an increase to approximately 20 kPa. The initial drop in pressure or 'lag' before observing a pressure increase can be attributed to the fact that the aluminium pile was

pushed into the augered hole from the top of the profile. Doing so resulted in slight disturbance of the adjacent soil, thereby creating a larger gap between the augered holes and the pile in the top layer. However, the general trend observed for all load cells is that an increase in lateral pressure occurs relatively early in the test, followed by a drop in pressure. This agrees with the results of Schreiner & Burland (1991) of an oedometer test with lateral stress measurement. It also supports the findings of Robertson & Wagener (1975) who observed that the maximum swell induced lateral pressure against abutment walls occurred before complete wetting was achieved.

The above finding also provides insights into the discrepancies in the publications of Blight (1984) and Elsharief (2007) mentioned earlier. While Blight (1984) and Elsharief (2007) reported an increase and reduction in shaft capacity respectively after wetting of the profile, neither author stated the magnitude of swell that had occurred at the time of testing. A closer investigation of these studies reveals wetting periods of 3-4 weeks (Blight, 1984) and 2 months (Elsharief, 2007). Considering the results in Fig. 15, it is likely that the tests conducted by Blight (1984) were conducted early in the swell process where there was still an increase in lateral swell pressure against the pile. Similarly, the significantly longer wetting period of Elsharief (2007) place the test in the later stages of the swelling process where swell induced softening becomes the dominant mechanism.

It is therefore crucial that any tests which aim to investigate the shaft capacity of a pile after swell has occurred, should be considered together with the anticipated magnitude of swell. By not considering the magnitude of anticipated swell, it cannot be stated whether softening or increases in lateral pressure will dominate the behaviour of the pile.

Even though the results presented in Fig. 15 are meant to provide qualitative illustrations of the variation in lateral stress, the result does at first, appear contradictory to the results of the plug pull-out tests presented previously. The end of the instrumented pile test represents the

level of swell at which plugs were pulled out of the profile for the previous tests. Whereas the result presented in Fig. 14 illustrates a relatively unchanged value of pull-out capacity for the bottom plug after swell when compared to the in-situ water content pull-out test, Fig. 15 illustrates a reduction in lateral stress in this clay layer. To reconcile these two results, it is important to consider the absolute values of stress throughout the model. The initial overburden stress at the bottom of the top layer and the bottom of the model is approximately 27 and 130 kPa respectively. As such, a unit reduction in lateral pressure at the latter stages of a swell process will have a much more significant impact on the shaft capacity in upper portions of the profile.

Conclusions

The results of the centrifuge tests presented in this study illustrate that the shaft (pull-out) capacity of a pile after allowing swell to occur is dependent on both overburden stress (depth in the profile) and on the magnitude of swell which has occurred. At the clay's in-situ water content, pull-out tests revealed no dependency of shaft capacity on overburden stress. However, after achieving a targeted value of swell (that predicted by Van der Merwe (1964) for a clay of very high potential expansiveness), a reduction in pull-out capacity was observed in the upper portions of the clay profile. This reduction in capacity can be attributed to swell-induced softening of the surrounding clay. Conversely, for short-length piles (plugs) tested at higher confining stresses, pull-out capacity remained relatively unchanged when compared to that measured under in-situ moisture conditions. An explanation for this finding is that at depth, where swell is largely restricted, so too are the effects of swell-induced softening.

In addition to the dependency on overburden stress, it was found that the change in lateral stresses against a pile is strongly dependent on the magnitude of heave which has occurred. Regardless of the position within a profile, lateral stresses tend to increase in the early stages of a swelling process and then reduce as heave continues. The lowest value of shaft resistance throughout the lifetime of a structure may either be at the clay's in-situ moisture

content, or after a significant magnitude of heave has occurred. If site tests are conducted to determine the shaft resistance of piles in expansive clays, an estimate of the likely magnitude of heave and its variation with depth during the lifetime of the structure is required to achieve a conservative design.

Acknowledgements

This work was funded by the UK Engineering and Physical Sciences Research Council (EPSRC) under the Global Challenges Fund programme for a project entitled 'Developing Performance based design for foundations of wind turbines in Africa (WindAfrica)', Grant Ref: EP/P029434/1. The first author would also like to acknowledge the Newton Fund UnsatPractice PhD exchange programme (grant Ref: ES/N013905/1), which enabled him to spend six months at Durham University during his PhD study at the University of Pretoria. The author's would also like to thank Corinus Claasen and Johan van Staden from Loadtech Loadcells (Centurion) who assisted with the manufacturing of the instrumented pile presented in this study.

Competing interests: The authors declare there are no competing interests.

Authors contribution statement:

Tiago Gaspar: Conceptualization; Methodology; Formal analysis; Investigation; Writing – Original Draft; Visualization

Schalk Jacobsz: Conceptualization; Supervision; Funding acquisition; Writing – Review & Editing; Project administration

Gerrit Smit: Conceptualization; Methodology; Writing – Review & Editing

Ashraf Osman: Conceptualization; Funding acquisition; Writing – Review & Editing; Project administration

Funding contribution statement: This research was supported by the UK Engineering and Physical Sciences Research Council (EPSRC) under the Global Challenges Fund programme

for a project entitled 'Developing Performance based design for foundations of wind turbines in Africa (WindAfrica)', Grant Ref: EP/P029434/1. The first author would also like to acknowledge the Newton Fund UnsatPractice PhD exchange programme (grant Ref: ES/N013905/1), which enabled him to spend six months at Durham University during his PhD study at the University of Pretoria.

Data availability statement: Data generated or analysed during this study are available from the corresponding author upon reasonable request.

References

ASTM (2014*a*). ASTM D854‐14: Standard Test Methods for Specific Gravity of Soil Solids by Water Pycnometer, West Conshohocken, P.A.

ASTM (2014*b*). ASTM D4546–14: Standard Test Method for One-Dimensional Swell or Collapse of Soils, Technical report, West Conshohocken, P. A.

ASTM (2017*a*). ASTM D6913 / D6913M-17: Standard Test Methods for Particle-Size Distribution (Gradation) of Soils Using Sieve Analysis, West Conshohocken, P.A.

ASTM (2017*b*). ASTM D7928-17: Standard Test Method for Particle-Size Distribution (Gradation) of Fine-Grained Soils Using the Sedimentation (Hydrometer) Analysis, West Conshohocken, PA.

ASTM (2017*c*). ASTM D4318-17e1: Standard Test Methods for Liquid Limit, Plastic Limit, and Plasticity Index of Soils, West Conshohocken, P. A.

ASTM (2017*d*). ASTM D2487-17e1: Standard Practice for Classification of Soils for Engineering Purposes (Unified Soil Classification System), West Conshohocken, P. A.

Blight, G. E. (1984). Power Station Foundations in Deep Expansive Soil Power Station Foundations in Deep Expansive Soil. *First International Conference on Case Histories in Geotechnical Engineering*, Missouri, pp. 77‐86.

Brackley, I. J. A. B. (1975*b*). A model of unsaturated clay structure and its application to swell behaviour. *Proceedings of the 6th African Regional Conference on Soil Mechanics and Foundation Engineering*, Vol. 1, pp. 65‐70.

Byrne, G., Chang, N. & Raju, V. (2019). A Guide to Practical Geotechnical Engineering in Africa, 5th Edition edn, FRANKI A KELLER COMPANY.

Charlie, W. A., Osman, M. A. & Elfatih, M. A. (1985). Construction on expansive soils in Sudan. Journal of Construction Engineering and Management, 110 No. **3**, 359-374

Day, P. (2017). Challenges and shortcomings in geotechnical engineering practice in the context of a developing country (Terzaghi Oration). *Proceedings of the 19th International Conference on Soil Mechanics and Geotechnical Engineering*, Seoul, pp. 11-34.

Elsharief, A. M., Ahmed, E. O. & Mohamedzein, Y. E. A. (2007). Guidelines for the Design of Bored Concrete Piles in Expansive Soils of Sudan. *Graduate School Conference, on Basic Sciences and Engineering*, University of Khartoum.

Elsharief, A. (2012). Foundations on Expansive Soils, Sudan Experience. *Graduate School Conference, on Basic Sciences and Engineering*, University of Khartoum.

Fleming, K., Weltman, A., Randolph, M. & Elson, K. (2009). Piling Engineering, 3rd edn, Taylor & Francis.

Fourie, A. B. (1991). Lateral swelling pressure developed in an active clay. *Geotechnics in the African Environment*, Maseru, Lesotho, (eds G. E. Blight, A. B. Fourie, I. Luker, D. J. Mouton & R. J. Scheurenberg), Vol. 1, pp. 267‑274 Balkema, Rotterdam, Maseru, Lesotho.

Fredlund, D. G. (1983). Prediction of ground movements in swelling clays. *31st Annual Soil Mechanics and Found Engineering Conference*. University of Minnesota, Minneapolis.

Gaspar, T. A. V., Jacobsz, S. W., Heymann, G., Toll, D. G., Gens, A., & Osman, A. S. (2022). The mechanical properties of a high plasticity expansive clay. *Engineering Geology*, *303*(March), 106647. https://doi.org/10.1016/j.enggeo.2022.106647

Gaspar, T. A. V., Jacobsz, S. W., Smit, G., Gens, A., Toll, D. G., & Osman, A. S. (2023). Centrifuge modelling of an expansive clay profile using artificial fissuring to accelerate swell. *Engineering Geology*, 312, 106928. https://doi.org/10.1016/j.enggeo.2022.106928

Gaspar, T.A.V. (2020). *Centrifuge modelling of piled foundations in swelling clays*. PhD Thesis, University of Pretoria, Pretoria, South Africa

Gens, A. & Alonso, E. E. (1992). A framework for the behaviour of unsaturated expansive clays. *Canadian Geotechnical Journal* **29**, No. 6, 1013–1032.

Jacobsz, S. W. (2002). The effects of tunnelling on piled foundations, PhD thesis, University of Cambridge September.

Jennings, J. E. & Kerrich, J. E. (1962). The heaving of buildings and the associated economic consequences with particular reference to the Orange Free State Goldfields. *The Civil Engineer in South Africa* **4** No. 11, 221‑248.

Li, J., Cameron, D. & Ren, G. (2014). Case study and back analysis of a residential building damaged by expansive soils. *Computers and Geotechnics*, **56**, 89‐99.

Louw, H., Kearsley, E., & Jacobsz, S. W. (2020). Modelling horizontally loaded reinforced-concrete piles in a geotechnical centrifuge. *International Journal of Physical Modelling in Geotechnics* **22** No.1, 14-25

Manca, D., Ferrari, A., & Laloui, L. (2016). Fabric evolution and the related swelling behaviour of a sand/bentonite mixture upon hydro-chemo-mechanical loadings. *Géotechnique*, *66*(1), pp. 41–57. https://doi.org/10.1680/jgeot.15.P.073

Monroy, R., Zdravkovic, L., & Ridley, A. M. (2015). Mechanical behaviour of unsaturated expansive clay under K0 conditions. *Engineering Geology*, *197*, pp. 112–131. https://doi.org/10.1016/j.enggeo.2015.08.006

Meintjes, H. A. C. (1991). A case history on heaving clay: Colinda Primary School. *Geotechnics in the African Environment*, Maseru, Lesotho, (eds G. E. Blight, A. B. Fourie, I. Luker, D. J. Mouton & R. J. Scheurenberg) pp. 99‐104.Balkema, Rotterdam.

Nelson, J. D., Reichler, D. K. & Cumbers, J. M. (2006). Parameters for heave prediction by oedometer tests. *Proceedings of the 4th International Conference on Unsaturated Soils*, Carefree, Arizona, pp. 951‐961.

Pellissier, J. P. (1997). A raft design method for swelling clay. *Proceedings of the 14th International Conference on Soil Mechanics and Foundations Engineering*. Hamberg, Germany, pp. 863‐869.

Robertson, A. & Wagener, F. (1975). Lateral swelling pressures in active clay. *Proceedings of the 6th African Regional Conference on Soil Mechanics and Foundation Engineering*, vol. 1, Durban, pp. 107‑114.

Schreiner, H. D. (1988). *Volume Change of Compacted Highly Plastic African Clays*, PhD thesis, Imperial College London.

Schreiner, H. D. & Burland, J. B. (1991). A comparison of three swell test procedures. *Geotechnics in the African Environment*, Maseru, Lesotho, (eds G. E. Blight, A. B. Fourie, I. Luker, D. J. Mouton & R. J. Scheurenberg), pp. 259‑266, Balkema, Rotterdam

Smit, G., Gaspar, T. A. V., Jacobsz, S. W. & Osman, A. S. (2019). Centrifuge modelling of pile pull-out tests in expansive soil*. XVII European Conference on Soil Mechanics and Geotechnical Engineering*, Reykjavik, Iceland.

Van der Merwe, D. (1964). The prediction of heave from the plasticity index and percentage clay fraction of soils. *The Civil Engineer* pp. 103‑107.